JOURNAL OF NATURAL PRODUCTS

pubs.acs.org/jnp

Article

Glycosides and Glycoconjugates of the Diterpenoid Isosteviol with a 1,2,3-Triazolyl Moiety: Synthesis and Cytotoxicity Evaluation

Olga V. Andreeva, Bulat F. Garifullin, Radmila R. Sharipova, Irina Yu. Strobykina, Anastasiya S. Sapunova, Alexandra D. Voloshina, Mayya G. Belenok, Alexey B. Dobrynin, Leysan R. Khabibulina, and Vladimir E. Kataev*

Cite This: https://dx.doi.org/10.1021/acs.jnatprod.0c00134

ABSTRACT: Several glycoconjugates of the diterpenoid isosteviol (16-oxo-*ent*-beyeran-19-oic acid) with a 1,2,3-triazolyl moiety were synthesized, and their cytotoxicity was evaluated against some human cancer and normal cell lines. Most of the synthesized compounds demonstrated weak inhibitory activities against the M-HeLa and MCF-7 human cancer cell lines. Three lead compounds, **54**, **56** and **57**, exhibited high selective cytotoxic activity against M-HeLa cells (IC_{50} = 1.7−1.9 μM) that corresponded to the activity of the anticancer drug doxorubicin (IC_{50} = 3.0 μM). Moreover, the lead compounds were not cytotoxic with respect to a Chang liver human normal cell line (IC_{50} > 100 μM), whereas doxorubicin was cytotoxic to this cell line (IC_{50} = 3.0 μM). It was found that cytotoxic activity of the lead compounds is due to induction of apoptosis proceeding along the mitochondrial pathway. The present findings suggest that 1,2,3-triazolyl-ring-containing glycoconjugates of isosteviol are a promising scaffold for the design of novel anticancer agents.

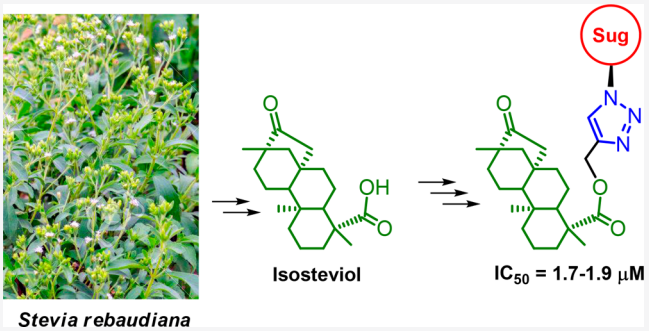

Cancer represents a major health problem facing the world and is responsible for 13% of all deaths worldwide according to the World Health Organization.[1] Despite the availability of a great number of chemotherapeutic drugs and other treatment modalities such as radiotherapy and surgery, cancer remains as one of the top five leading causes of mortality globally.[2] Successfully curing cancer still represents a great problem. Chemotherapeutic drugs, in having been used in therapy for several years, suffer from several disadvantages such as severe toxicity, nonselectivity (normal versus cancer cells), and drug resistance.[3,4] Furthermore, such compounds may generate severe side effects associated with their necrotic activity, a fact that indicates the need to seek new compounds, with high antiproliferative activity but low necrotic effects that are capable of inducing apoptosis of cancer cells. Moreover, overcoming resistance to apoptosis by activating apoptosis pathways has been a major focus in the development of therapeutic strategies for cancer treatment.[5]

The tetracyclic diterpenoid isosteviol (**1**, 16-oxo-*ent*-beyeran-19-oic acid[6]) is obtained readily by acid hydrolysis of the *Stevia rebaudiana* (Bertoni) Bertoni (Asteraceae) glycoside stevioside,[7] a component of various low-calorie sweeteners manufactured on a large scale in a number of countries.[8] Isosteviol (**1**) exhibits a broad range of bioactivities, including antituberculosis,[9b] antihyperglycemic,[9c] cardioprotective,[9d] antihypertensive,[9e] and antimicrobial effects.[9i] Moreover, compound **1** has been found to inhibit in vivo chemically induced mouse skin carcinogenesis[9f] and to demonstrate cytotoxicity against MOLT-4 T-lymphoblastic leukemia cells,[9a] BALL-1 B-lymphoblastic leukemia cells,[9a] NUGC-3 human gastric cells,[9a] and HL60 human leukemia cells.[9g] Numerous chemical modifications of isosteviol (**1**) have furnished a large series of derivatives that showed similar activities to those listed above[9n] and also have antiviral,[9j] antimitotic,[9k] and mitochondriotropic effects.[9m]

Recently, we have synthesized a series of glycosides and glycoconjugates of isosteviol (**1**), which showed moderate to potent cytotoxicity against several human cancer cell lines.[9p,q] In continuation of this study, herein are described the synthesis and cytotoxicity evaluation of 1,2,3-triazolyl-ring-containing glycoconjugates of isosteviol (**1**).

RESULTS AND DISCUSSION

Chemistry. The synthesis of 1,2,3-triazolyl-ring-containing glycoconjugates of isosteviol (**1**) was performed by a

Received: February 6, 2020

Scheme 1. Terpenoid Route of Convergent Synthesis

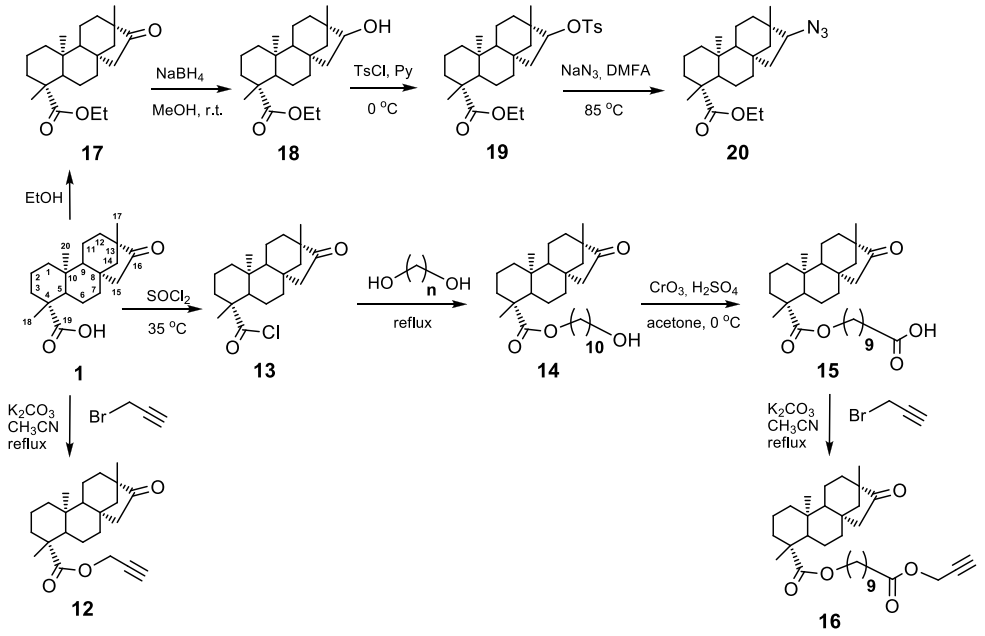

convergent scheme consisting of terpenoid and carbohydrate routes completed with the formation of terpenoid and carbohydrate precursors that are alkyne and azido derivatives of **1** and several monosaccharides. At the final stage of the convergent scheme, the precursors were coupled by a copper-catalyzed azide−alkyne cycloaddition (CuAAC) reaction, to afford the target 1,2,3-triazolyl-ring-containing glycoconjugates of **1**. The terpenoid route focused on the synthesis of isosteviol precursors **12**, **16**, and **20**, bearing a terminal alkyne bond or an azide group (Scheme 1).

First, isosteviol (**1**) was alkylated with propargyl bromide in acetonitrile at reflux in the presence of potash to afford the precursor **12** in 98% yield, as reported earlier[9h] (Scheme 1). Second, the reaction of the in situ-generated chloroanhydride **13** with 1,10-decanediol afforded oxoalcohol **14** in 57% yield.[9o] Then, the hydroxy group of **14** was oxidized with Jones' reagent, and the corresponding oxoacid **15** was obtained in 93% yield[9o] and was engaged in an alkylation with propargyl bromide to afford the precursor **16** in 89% yield (Scheme 1). The azido precursor **20** was prepared in four steps by analogy with a procedure already described.[9l] Isosteviol ethyl ester (**17**) subsequently was converted first to the 16α-hydroxy derivative **18** then to the 16α-tosylate **19**. The reaction of compound **19** with NaN_3 in dry DMF furnished the desired azido precursor **20** in 92% yield (Scheme 1).The absolute configuration of compound **20** was confirmed by X-ray crystallographic analysis and demonstrated a β-orientation of the azido group at C-16 (Figure 1).

The carbohydrate route consisted of five independent parts: syntheses of the precursors on the basis of D-glucopyranose, D-galactopyranose, *N*-acetyl-D-glucosamine, D-ribose, and D-arabinofuranose.

The precursors based on D-glucopyranose (**24**, **25**, and **28**) (Scheme 2) were prepared by analogy with the methods previously described.[10] 1,2,3,4,6-Penta-*O*-acetyl-β-D-glucopyranose (**22**), obtained by acetylation of D-glucopyranose (**21**) with Ac_2O in pyridine,[10b] was treated with a solution of HBr in acetic acid to afford the acetyl-protected 1-bromo glucopyranoside (**23**).[10c] The crude product was used in the reaction with

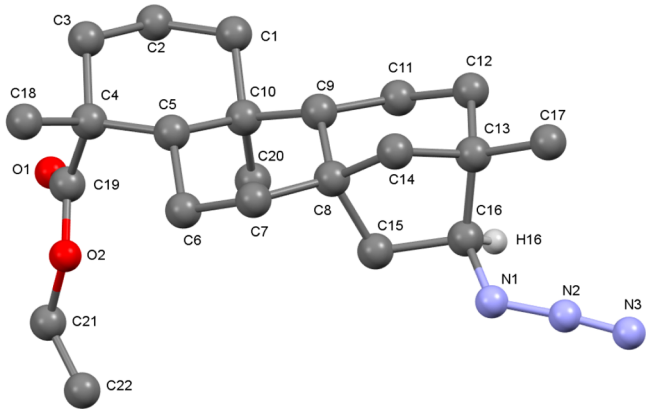

Figure 1. X-ray structure of compound **20**.

sodium azide without any purification to obtain 2,3,4,6-tetra-*O*-acetyl-β-D-glucopyranosyl azide (**24**)[10a] in 66% yield. Then, the acetyl protective groups were removed with a solution of NaOMe in MeOH[10e] to provide the azido precursor **25** in 99% yield.

The hemiacetal **26**, obtained by the anomeric deprotection of the pentaacetylated D-glucopyranose (**22**) with a solution of hydrazine hydrate in acetic acid,[10d] was used in a reaction with trichloroacetonitrile[10f] to afford 2,3,4,6-tetra-*O*-acetyl-β-D-glucopyranosyl trichloroacetimidate (**27**) in 35% yield. The reaction of compound **27** with propargyl alcohol in the presence of trimethylsilyltrifluoromethanesulfonate (TMSOTf)[10f] then gave 1-*O*-propargyl-2,3,4,6-tetra-*O*-acetyl-β-D-glucopyranose (**28**) in 82% yield. The precursor using D-galactose **32**[10a] was prepared in three steps by full analogy with the azido precursor **25**, in 44% yield (Scheme 3).

The precursors related to the *N*-acetyl-D-glucosamine derivatives **36** and **40** were obtained by a methodology previously described[11] (Scheme 4). A suspension of D-glucosamine hydrochloride (**33**) in a mixture of methanol and sodium methoxide was treated with acetic anhydride to give *N*-acetyl-D-glucosamine (**34**).[11a] Then, the reaction of

https://dx.doi.org/10.1021/acs.jnatprod.0c00134
J. Nat. Prod. XXXX, XXX, XXX−XXX

Scheme 2. Carbohydrate Route of Convergent Synthesis. Precursors Using D-Glucopyranose

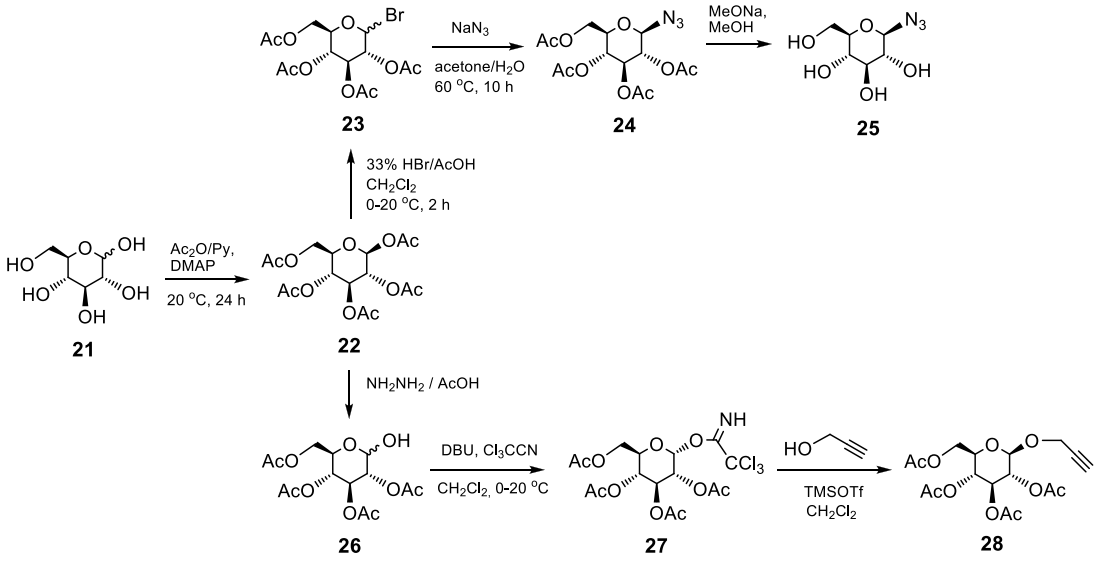

Scheme 3. Carbohydrate Route of Convergent Synthesis. Precursors Using D-Galactopyranose

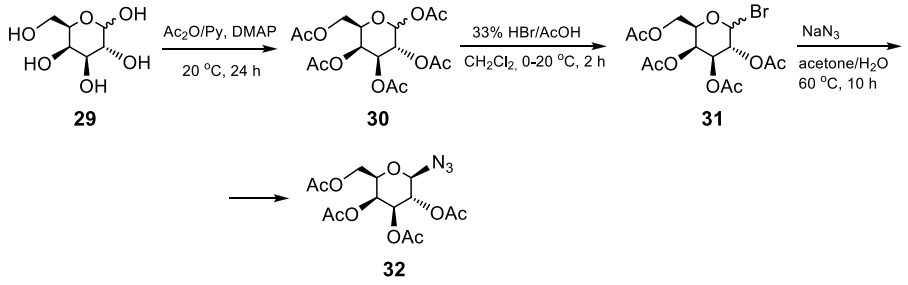

Scheme 4. Carbohydrate Route of Convergent Synthesis. Precursors Using *N*-Acetyl- D-glucopyranose

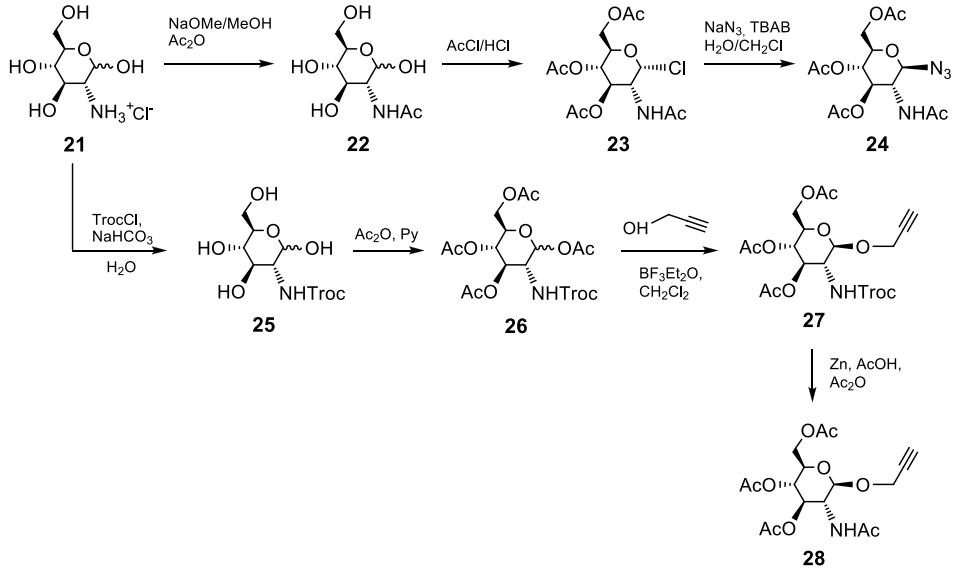

compound **34** with acetyl chloride in the presence of dry hydrogen chloride provided 2-deoxy-2-acetamido-3,4,6-tri-*O*-acetyl-*α*-D-glucopyranosyl chloride (**35**),[11b] which was treated with sodium azide in the presence of tetra-*n*-butylammonium bromide (TBAB) to afford 2-deoxy-2-acetamido-3,4,6-tri-*O*-acetyl-*β*-D-glucopyranosyl azide (**36**) in 57% yield.[11e] In the next step, 2,2,2-trichloroethoxycarbonyl chloride (TrocCl) was added to D-glucosamine hydrochloride (**33**) in saturated aqueous $NaHCO_3$ to obtain *N*-(2′,2′,2′-trichloroethoxycarbonyl)-D-glucosamine (**37**),[11c] which then was treated with acetic anhydride in pyridine to give 1,3,4,6-tetra-*O*-acetyl-*N*-(2′,2′,2′-trichloroethoxycarbonyl)-D-glucosamine (**38**).[11c] The reaction of compound **38** with propargyl alcohol in the presence of $BF_3{\cdot}OEt_2$ gave 3,4,6-tri-*O*-acetyl-*N*-(2′,2′,2′-

https://dx.doi.org/10.1021/acs.jnatprod.0c00134
J. Nat. Prod. XXXX, XXX, XXX−XXX

Scheme 5. Carbohydrate Route of Convergent Synthesis. Precursors Using D-Ribofuranose and D-Ribopyranose

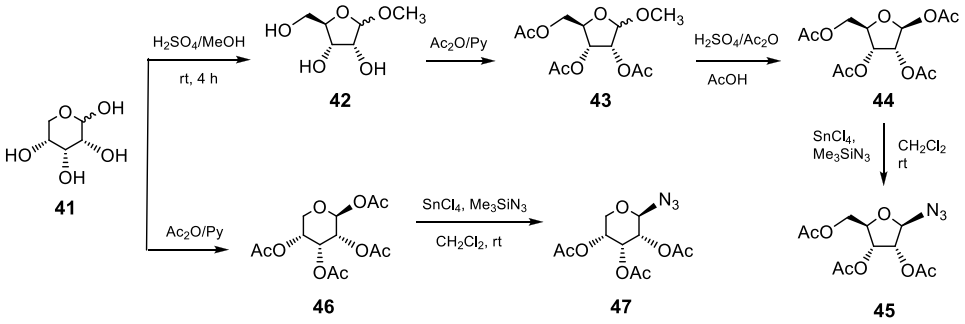

Scheme 6. Carbohydrate Route of Convergent Synthesis. Precursors Using D-Arabinofuranose

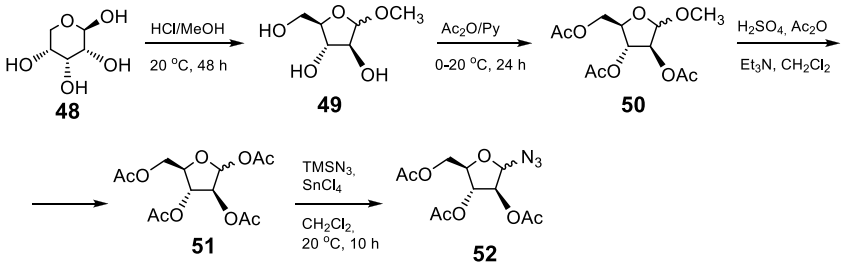

trichloroethoxycarbonyl)-1-*O*-(2′-propargyl)-*β*-D-glucosaminide (**39**), which was treated with zinc powder in acetic acid without purification. When the reaction was completed, acetic anhydride was added to the reaction mixture to afford *N*-acetyl-3,4,6-tri-*O*-acetyl-1-*O*-(2′-propargyl)-*β*-D-glucosaminide (**40**) in 98% yield.[11d]

The precursor using D-ribofuranose (**45**) was synthesized according to a known procedure.[12b] The treatment of a solution of the commercially available D-ribose (**41**) in MeOH with H_2SO_4, followed by acetylation with Ac_2O in pyridine, gave methyl 2,3,5-tri-*O*-acetyl-*α*/*β*-D-ribofuranoside (**43**) (Scheme 5). A solution of the crude product **43** in glacial AcOH and Ac_2O was reacted with H_2SO_4 to provide 1,2,3,4-tetra-*O*-acetyl-D-ribose as a mixture of *α*- and *β*-anomers, which were separated by flash chromatography on a silica gel column to afford the pure *β*-anomer **44** in 45% yield. Then, the reaction of compound **44** with trimethylsilyl azide in the presence of $SnCl_4$ resulted in precursor **45**[12a] in 95% yield. The treatment of commercially available D-ribose with an excess of Ac_2O in pyridine gave 1,2,3,4-tetra-*O*-acetyl-*β*-D-ribopyranose (**46**), which was engaged in a reaction with trimethylsilyl azide in the presence of tin tetrachloride to provide the azido precursor **47**[12a] in 99% yield (Scheme 5). The precursor **52** using D-arabinofuranose was synthesized by full analogy with precursor **45**[12a] with D-ribose, in 80% yield (Scheme 6).

Finally, CuAAC was utilized to complete the convergent synthesis and couple the carbohydrate azido precursors **24**, **32**, **36**, **45**, **47**, and **52** with the alkyne derivative of isosteviol **12** (Scheme 7). The CuAAC reactions were performed in *t*-BuOH/H_2O (1:1) using equimolar amounts of the reactants, $CuSO_4{\cdot}5H_2O$ (10 mol %) and sodium ascorbate (20 mol %). These conditions were found to be optimum in terms of the solvent and the amount of catalyst.[13] The desired 1,2,3-triazolyl-ring-containing glycoconjugates of isosteviol with protected OH groups of the sugar residues (**53**−**58**) were obtained in excellent yields (92−98%). The formation of the 1,2,3-triazole ring was indicated by the presence in the ^{1}H NMR spectra of **53**−**58** of the signal for the triazolyl proton H-5″ within the range 7.73−7.88 ppm. The triazolyl C-4″ carbons in their ^{13}C NMR spectra resonated within the range 143.1−143.6 ppm, and the signals of triazolyl C-5″ carbons were observed within the range 122.1−123.3 ppm.

The structures obtained were in full accordance with the characteristic features of the ^{1}H and ^{13}C NMR spectra of 1,2,3-triazoles previously described in the literature.[13a,14] It is worth noting that the CuAAC reactions provided 1,2,3-triazolyl-ring-containing glycoconjugates **53**−**57** with *β*-oriented glycosidic bonds, as evident from their ^{1}H NMR spectra. The anomeric protons of the acetylated sugar moieties of compounds **54**−**56** were observed in the ^{1}H NMR spectra as doublets within the range 5.83−6.10 ppm with vicinal coupling constants between 9.1 and 10.0 Hz, consistent with literature values.[9p,q] The anomeric proton of the 2,3,4,6-tetra-*O*-acetyl-*β*-D-glucopyranosyl residue in the glycoconjugate **53** resonated as a multiplet at 5.84−5.89 ppm in accordance with the literature.[15] The ^{1}H NMR spectrum of **57** showed the anomeric proton as a doublet at 6.13 ppm with a vicinal coupling constant of 3.8 Hz, indicating a *β*-orientation of the glycosidic bond, again as expected.[12b] The only glycoconjugate (**58**) having a 2,3,5-tri-*O*-acetyl-D-arabinofuranose residue, as well as its azido precursor **52**, was obtained as the *α*-anomer. The anomeric proton of compound **52** resonated in the ^{1}H NMR spectrum as a singlet at 5.45 ppm as in the literature,[12a] and the anomeric proton of compound **58** in its ^{1}H NMR spectrum was observed as a doublet at 6.12 ppm (^3J = 1.7 Hz).[15a] Finally, the removal of the *O*-acetyl protective groups of **53**−**58** with 0.1 N MeONa/MeOH solution furnished the desired 1,2,3-triazolyl glycoconjugates of isosteviol **59**−**64** bearing unprotected OH groups in good yields (83−96%). The absolute configuration of compound **53** was determined by X-ray crystallographic analysis (Figure 2).

To evaluate how cytotoxicity might be altered on moving of the 1,2,3-triazolyl sugar residue away from the isosteviol skeleton, glycoconjugates **65** and **66** were synthesized by coupling the alkyne derivative of isosteviol **16** and azido precursors **24** and **25** under CuAAC conditions, in 96% and

https://dx.doi.org/10.1021/acs.jnatprod.0c00134
J. Nat. Prod. XXXX, XXX, XXX−XXX

Scheme 7. Synthesis of 1,2,3-Triazolyl Glycoconjugates of Isosteviol

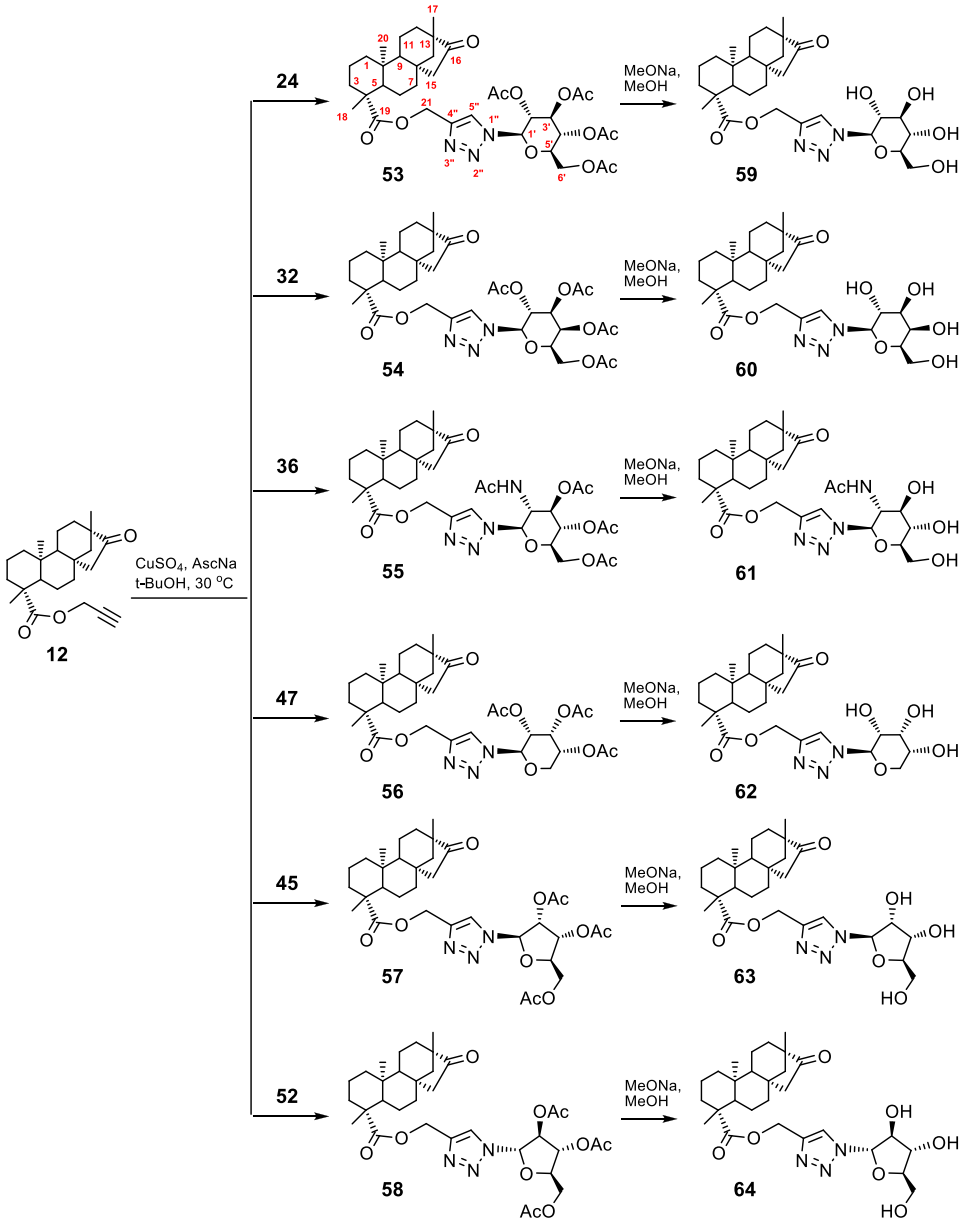

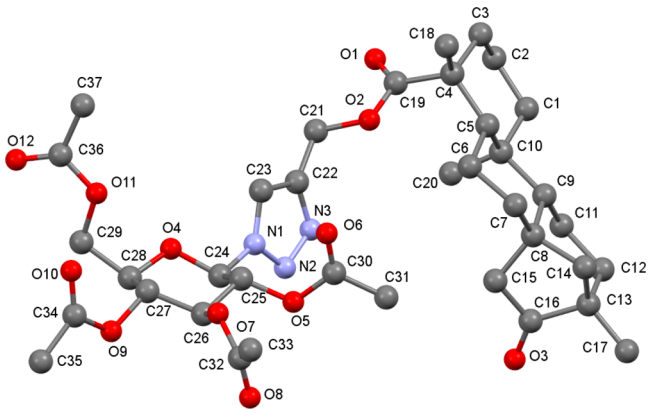

Figure 2. X-ray structure of compound **53**.

Scheme 8. Synthesis of 1,2,3-Triazolyl Glycoconjugates 65 and 66

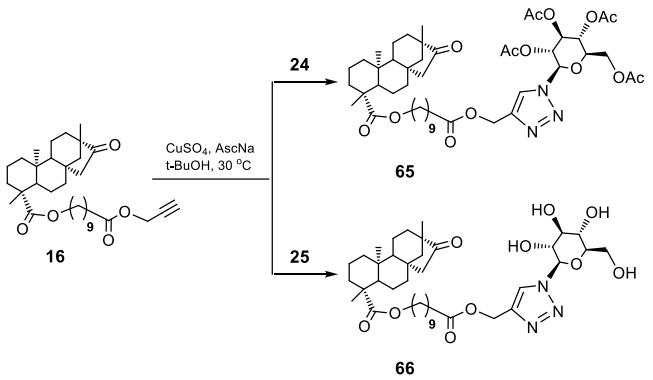

95% yields, respectively (Scheme 8). The presence in the ^{1}H NMR spectra of **65** and **66** of singlets at 7.82 and 7.78 ppm (H-5″), respectively, as well as the presence in the ^{13}C NMR spectrum of **65** of signals at 143.84 ppm (C-4″) and 122.01

https://dx.doi.org/10.1021/acs.jnatprod.0c00134
J. Nat. Prod. XXXX, XXX, XXX−XXX

Table 1. Cytotoxic Activity of 1,2,3-Triazolyl Ring-Containing Glycoconjgates of Isosteviol against Human Cancer and Human Normal Cell Lines (IC_{50} Values in μM with Standard Errors)[a]

compound	structure	IC_{50} (μM)				SI[e]
		cancer cell lines		normal cell lines		
		M-HeLa[b]	MCF-7[c]	Wi-38[d]	Chang liver	
53	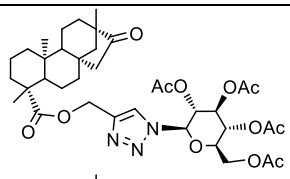	8.0±0.7	>10	36.0±3.0	68.3±5.4	8.5
54	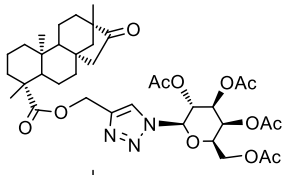	1.8±0.14	>10	69.7±6.1	>100	>56
56	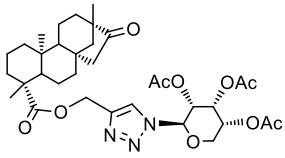	1.7±0.15	>10	40.0±3.1	>100	>59
57	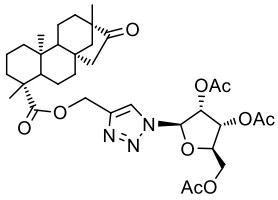	1.9±0.15	>10	>100	>100	>53
doxorubicin		3.0±0.2	3.0±0.1	1.3±0.09	3.0±0.1	1.0

[a]The experiments were repeated three times. [b]M-HeLa is a human cervix epitheloid carcinoma. [c]MCF-7 is a human breast adenocarcinoma (pleural fluid). [d]Wi-38 is a diploid human cell strain composed of fibroblasts derived from the lung tissue of a 3-month-gestation-aborted female fetus. [e]Selectivity index calculated as the ratio between the IC_{50} value on Chang liver cells and the IC_{50} value on M-HeLa cells.

ppm (C-5′′), and the presence of signals at 144.22 ppm (C-4′′) and 125.12 ppm (C-5′′) in the ^{13}C NMR spectrum of **66** proved the formation of the 1,2,3-triazole ring according to the literature data.[13a,14] The anomeric protons of glycoconjugates **65** and **66** resonated in the ^{1}H NMR spectra as a multiplet at 5.85−5.89 ppm for **65** and a doublet at 5.60 ppm (^{3}J = 9.3 Hz) for **66**, which confirmed the β-orientation of the glycosidic bonds, in conformity with published values.[9p,q,15]

To determine how cytotoxicity might change upon transfer of the 1,2,3-triazolyl sugar residue from the ester group of isosteviol to ring D, azido precursor **20** was engaged in a CuAAC reaction with carbohydrate precursors **28** and **40** to afford glycoconjugates **67** and **68** in yields of 79% and 69%, respectively. The formation of the 1,2,3-triazole rings was indicated by the presence in the ^{1}H NMR spectra of **67** and **68** of the signal for the triazolyl H-5″ proton at 7.43 and 7.47 ppm, respectively. The triazolyl C-4′′ carbon in the ^{13}C NMR spectra of **67** and **68** resonated at 143.45 and 143.84 ppm, respectively, and the triazolyl C-5″ carbon occurred at 122.36 and 122.41 ppm, respectively. These data were in full accordance with characteristic features of the ^{1}H and ^{13}C NMR spectra of 1,2,3-triazoles previously described.[13a,14] The removal of the *O*-acetyl protective groups of **67** and **68** with a 0.1 N MeONa/MeOH solution afforded 1,2,3-triazolyl glycoconjugates of isosteviol **69** and **70** in 80% and 81% yields, respectively.

Cytotoxicity of 1,2,3-Triazolyl Glycoconjugates of Isosteviol toward Cancer Cells. The target 1,2,3-triazolyl glycoconjugates of isosteviol (**53**−**70**) were subjected to evaluation for cytotoxicity against two human cancer cell lines [cervical epitheloid carcinoma (M-HeLa) and breast adenocarcinoma (MCF-7)], as well as the Chang liver normal human cell line and a diploid human cell strain WI-38 composed of fibroblasts. Only four 1,2,3-triazolyl glycoconjugates, namely, **53**, **54**, **56**, and **57**, showed good activity against M-HeLa cells, and the activity of compounds **54**, **56**, and **57** corresponded to the activity of the anticancer drug doxorubicin (Table 1). As to the cytotoxicity of these glycoconjugates against MCF-7 cells, they were approximately 20 times less potent than doxorubicin. The cytotoxicities of other 1,2,3-triazolyl glycoconjugates of isosteviol synthesized in this study were lower, with IC_{50} values of >10 μM. To evaluate the efficiency of the lead compounds **54**, **56**, and **57**, selectivity indexes (SI) were calculated as the ratio IC_{50}(Chang liver)/IC_{50}(M-HeLa) (Table 1).

Induction of Apoptotic Effects by Compounds 54, 56, and 57. To establish whether the observed cytotoxicity of the lead compounds **54**, **56**, and **57** is associated with the induction of apoptosis, an annexin V-FITC/PI double stain

https://dx.doi.org/10.1021/acs.jnatprod.0c00134
J. Nat. Prod. XXXX, XXX, XXX−XXX

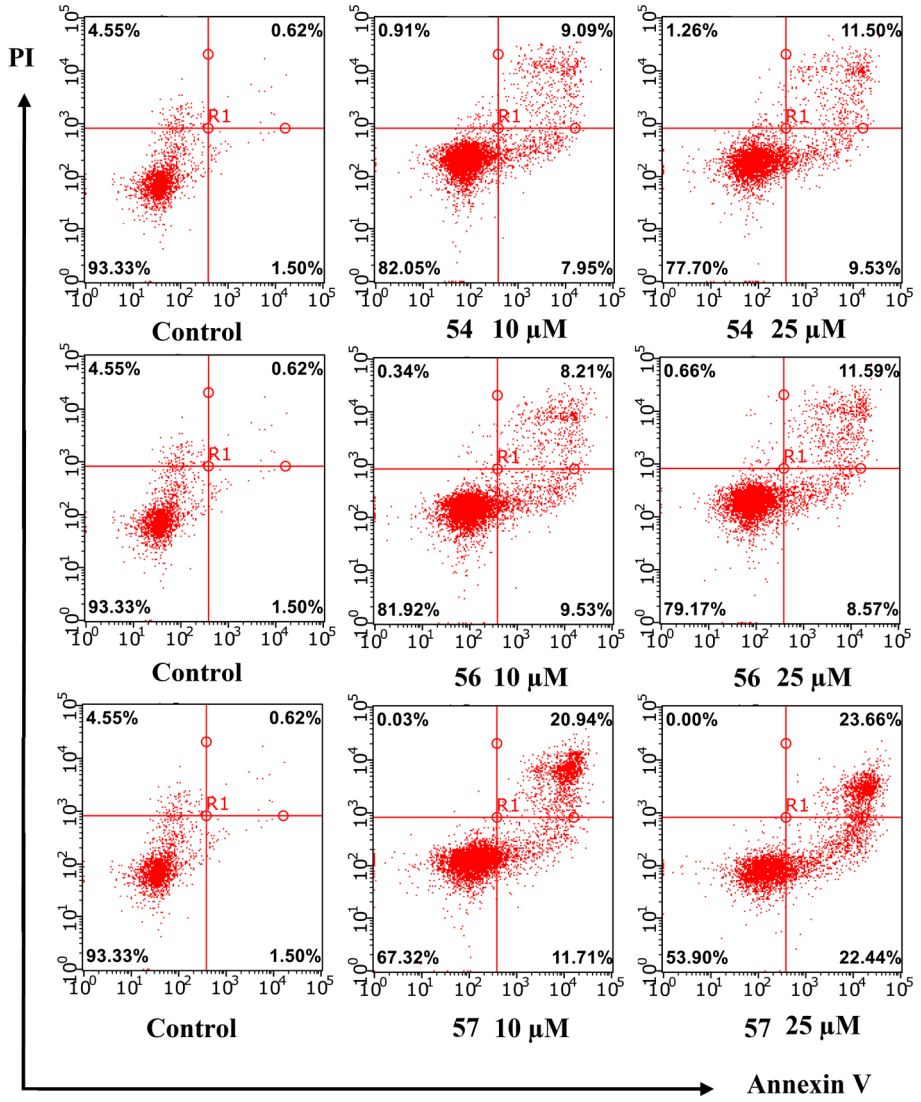

Figure 3. Apoptotic effects of compounds **54**, **56**, and **57** on M-HeLa cells. (A) M-HeLa cells were treated with these compounds at the indicated concentrations for 24 h. Apoptotic effects were measured by flow cytometry using the annexin V-FITC staining protocol. The values are presented as means ± SD (n = 3).

analysis was performed after treatment of M-HeLa cells. As shown in Figure 3, after 24 h of treatment, significant apoptotic effects were observed for all three compounds in M-HeLa cells. Analysis of apoptotic effects (Figures 3 and 4) showed that after incubation of cells with compounds **54** and **56** at a concentration of 10 μM, the number of cells during early and late apoptosis did not differ significantly. With an increase in the concentration of compounds **54** and **56** to 25 μM, the number of cells with late apoptosis increased. The apoptotic effects caused by compound **57** differed from those for compounds **54** and **56**. At a concentration of 10 μM, the number of cells in late apoptosis was over two times greater than in early apoptosis (29.94% and 11.71%, respectively). With an increase in the concentration of compound **57** to 25 μM, the number of M-HeLa cells in early and late apoptosis became approximately the same. Thus, the results obtained showed that the cytotoxicity of compounds **54**, **56**, and **57** in cancer cells of M-HeLa is due to their effects on an apoptotic pathway.

Effects on the Mitochondrial Membrane Potential ($\Delta\psi_m$) by Compounds 54, 56, and 57. Next, the possible mechanism of action of the lead compounds **54**, **56**, and **57** on cancer cells was investigated, and their ability to cause a decrease in mitochondrial membrane potential ($\Delta\psi_m$) evaluated in M-HeLa cells by flow cytometry using JC-10 reagent. In normal cells with a high mitochondrial membrane potential, the dye JC-10 forms aggregates (J-aggregate) near mitochondrial membranes. When the membrane potential, due to the stimulation of apoptosis, falls, JC-10 is evenly distributed in the cell as a monomer (J-monomer). In normal cells JC-10 aggregates have a red fluorescence, while JC-10 monomers are green. The ratio between orange-red and green fluorescence can be used to judge the onset of apoptosis. A reduction in $\Delta\psi_m$ was demonstrated using flow cytometry analysis (Figures 5 and 7). The intensity of the red fluorescence decreased with increasing the concentration of the test compound. The results obtained suggest that the mechanism of action of the lead compounds **54**, **56**, and **57** can be associated with the induction of apoptosis that proceeds along a mitochondrial pathway.

The molecular mechanisms of apoptosis induced by the lead compound **54** were studied using the Milliplex MAP 7-plex

https://dx.doi.org/10.1021/acs.jnatprod.0c00134
J. Nat. Prod. XXXX, XXX, XXX−XXX

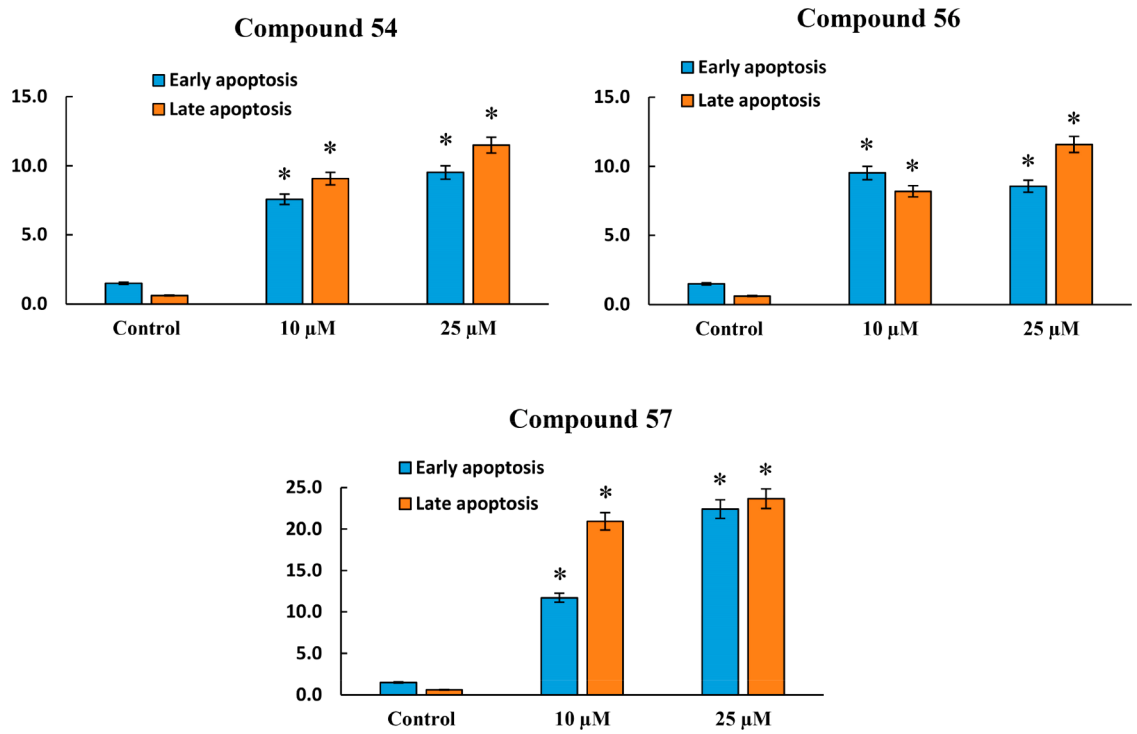

Figure 4. Representative histograms for the numbers of cells (% of total) in the early and late stages of apoptosis for the control and compounds **54**, **56**, and **57**. The values are presented as means ± SD (n = 3): (*) p < 0.01 compared to control.

early phase apoptosis signaling kit, which enables changes to be evaluated in the content of seven classical markers of early apoptosis (Akt, JNK, Bad, Bcl-2, p53, caspase-8, and caspase-9) with the help of the Luminex technology. Early apoptosis markers were detected in lysates of M-HeLa cells cultured in the presence of compound **54** at a concentration of 10 μM. As a control, M-HeLa cells not treated with the test compound were used. The change in the content of early apoptosis markers was evaluated by the difference in the mean fluorescence intensity (MFI) values in the test and control samples. Figure 7 shows that the fluorescence intensity of caspase-9 in the experimental sample was two times higher than in the control. The data obtained indicated that apoptosis proceeds along the internal pathway of caspase-9 activation, in which cell death occurs due to mitochondrial dysfunction and not along the external pathway associated with caspase-8 activation, since the fluorescence intensity remained unchanged in the experimental and control samples. This inference was confirmed by the predominance of anti-apoptotic Bcl-2 proteins responsible for irreversible cell damage in mitochondrial processes over pro-apoptotic Bad proteins.

Mitochondrial damage can also be caused by the tumor protein p53, the effect of which is manifested in the presence of Akt protein kinase. The fluorescence intensity of these markers in the test sample was higher than in the control. Apoptosis can also be caused by a stress that cells experience as a result of exposure to the test compound. This is evidenced by an increase in the JNK protein, known as the C-Jun N-terminal kinase or stress-activated protein kinase. Thus, one can conclude that the lead compound **54** has a cytotoxic effect due to the induction of apoptosis that proceeds along the mitochondrial pathway.

Target Selection and Molecular Docking. Thus, glycoconjugates of diterpenoid isosteviol (**1**) with a 1,2,3-triazolyl moiety inhibited the growth of the M-HeLa human cervix epitheloid carcinoma cell line. The cervix uteri tissue is very sensitive to the effects of sex hormones.[16a] Endo- and exogenous hormones capable of interacting with the estrogen receptor[16f] play an important role in the development of cervical cancer.[16b,e] Therefore, it is perhaps not surprising that selective estrogen receptor modulators (SERMs) such as raloxifene and fulvestrant are used to treat this type of cancer.[16c] SERMs are estrogen mimetics and selectively bind with the estrogen receptor.[16d] Glycosides for which the aglycone is an estrogen mimetic can also serve as SERMs.[16g] The *ent*-beyerane framework of isosteviol and the estrane framework of estradiol have a common perhydrophenanthrene motif. It was suggested that this similarity is the reason that permits the lead compounds **54**, **56**, and **57** to bind selectively to the estrogen receptor. Therefore, it was decided to test this possibility by evaluating the energy of their binding in the ligand-binding center (LBD) of the estrogen receptor (ERα) in molecular docking simulations.

Binding with the estrogen receptor (PDB code 5TM8) was evaluated for the lead compounds **54**, **56**, and **57**, which showed the best cytotoxicity against the M-HeLa cell line. These compounds exhibited approximately the same high binding energy in the ligand-binding domain of ERα ranging from −9.3 to −9.6 kcal/mol (Table 2). The positions of the optimized docking model of compounds **54**, **56**, and **57** and their two-dimensional interaction map into the ERα binding site are shown in Figure 8. All compounds had a very similar binding mode. In all cases, the carbohydrate moiety is in the depth of the binding pocket and the isosteviol moiety is retained in the cavity by hydrophobic interactions with the residues Leu525, Met528, Lys529, Leu536, Leu541, and

https://dx.doi.org/10.1021/acs.jnatprod.0c00134
J. Nat. Prod. XXXX, XXX, XXX−XXX

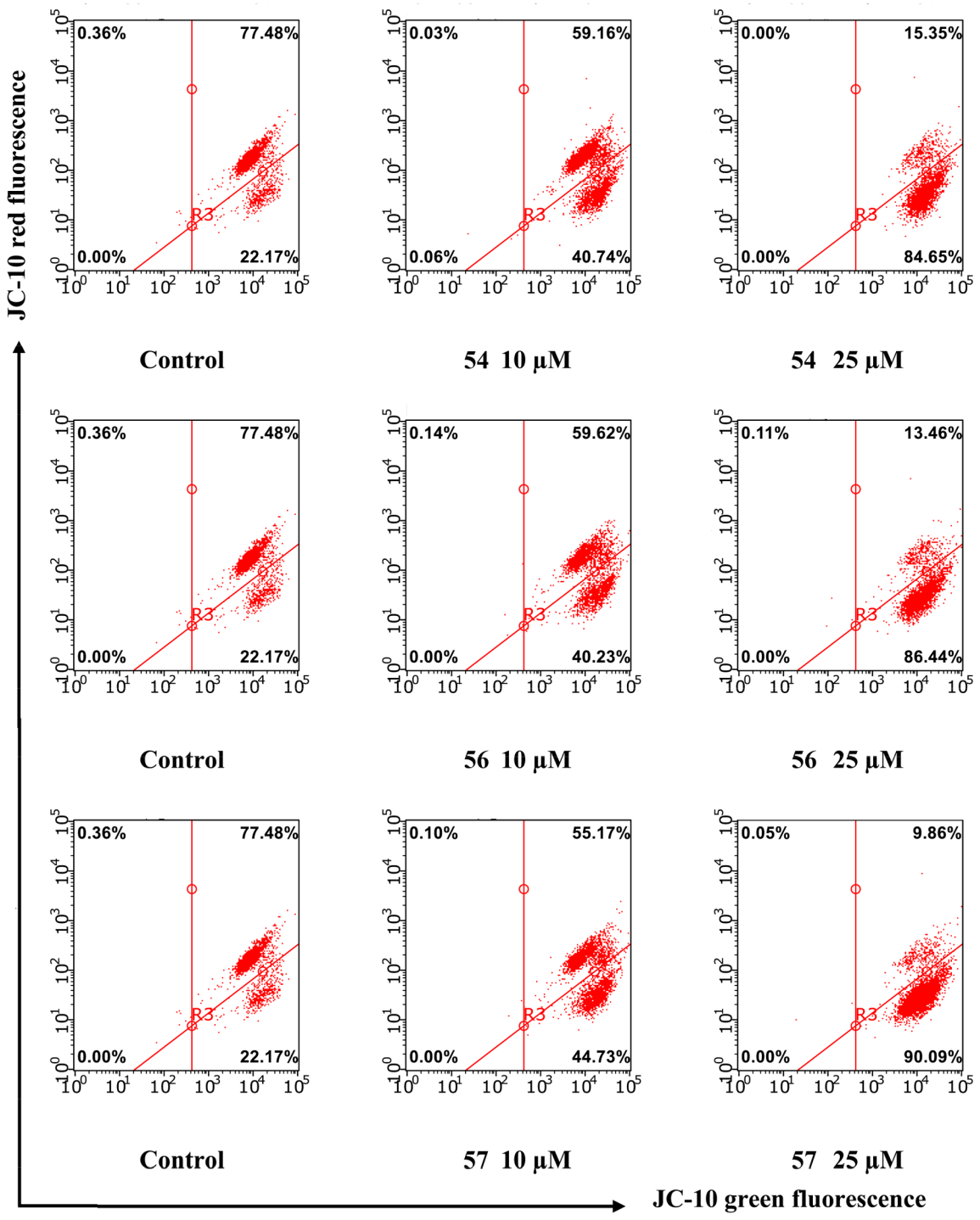

Figure 5. Flow cytometry analysis of M-HeLa cells treated with the lead compounds **54**, **56**, and **57**.

Leu544. In addition, the retention of ligands in the mouth of the binding pocket in all three cases is ensured by hydrogen bonding of the C═O bond of isosteviol with the Pro535 residue. Thus, molecular docking simulations demonstrated the ability of compounds **54**, **56**, and **57** to bind to the LBD of ERα that allows this protein to be considered as a potential molecular target, for which this interaction ensures their cytotoxicity against the M-HeLa cell line. This observation may help rationalize the search for potential drugs for treating cervical cancer among isosteviol glycoconjugates in future work.

EXPERIMENTAL SECTION

Synthesis of the Protected 1,2,3-Triazolyl Ring-Containing Glycoconjugates of Isosteviol (53−58). These compounds were synthesized according to Scheme 7. To a solution of equimolar amounts of propynyl 16-oxo-*ent*-beyeran-19-oate (**12**) and the protected azido derivatives of each of monosaccharides **24**, **32**, **36**, **45**, **47**, and **52** in a mixture of 1:1 *tert*-butanol/water was added a freshly prepared solution of equimolar amounts of sodium ascorbate in 2 mL of water and $CuSO_4 \times 5\ H_2O$ in 2 mL of water. The reaction mixture was stirred at 40 °C for 48 h and was concentrated under reduced pressure. The residue was taken up in methylene chloride, washed with water, dried over anhydrous sodium sulfate, and

https://dx.doi.org/10.1021/acs.jnatprod.0c00134
J. Nat. Prod. XXXX, XXX, XXX−XXX

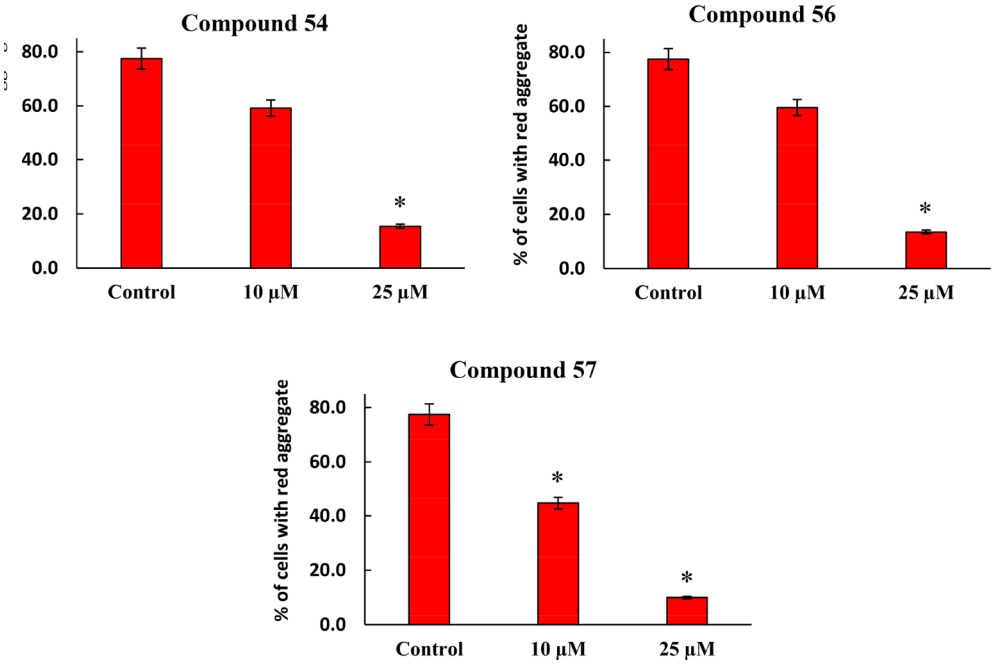

Figure 6. Quantitative determination of % cells with red aggregates. Values are presented as means ± SD (n = 3): (*) p < 0.01 compared to control.

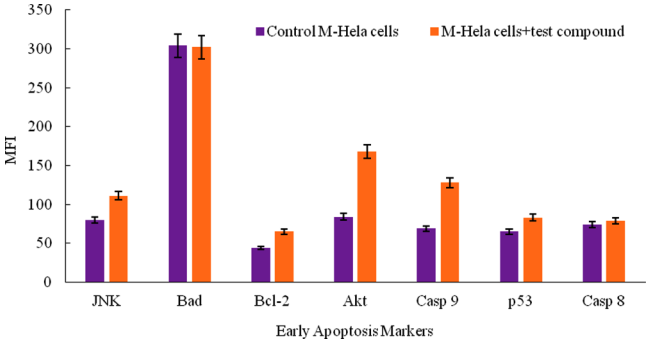

Figure 7. Multiplex analysis of early apoptosis markers in M-HeLa cells treated with the lead compound **54** at a concentration of 10 μM. M-HeLa cells without treatment by compound **54** were used as the control. Average fluorescence intensity (MFI) was measured using the Luminex system. The experiment was carried out three times.

concentrated under vacuum to provide the desired 1,2,3-triazolyl-ring-containing glycoconjugates **53**−**58** with acetylated sugar residues in 87−98% yields (Supporting Information). The products were characterized by ^{1}H NMR, ^{13}C NMR, MALDI MS, and elemental analysis data (Supporting Information).

Synthesis of the Unprotected 1,2,3-Triazolyl Ring-Containing Glycoconjugates of Isosteviol (59−64). These compounds were synthesized according to Scheme 7. The protected 1,2,3-triazolyl-ring-containing glycoconjugates **53**−**58** were dissolved in anhydrous MeOH at room temperature, and the pH was adjusted to 9.0 using a solution of 0.1 N MeONa/MeOH. The deacetylation procedure was monitored by TLC, and upon its completion the pH adjusted to 7.0 with the acidic ion-exchange resin Amberlyst 15. After filtration, the filtrate was concentrated under reduced pressure to afford the corresponding target compounds **59**−**64** in 88−95% yields (Supporting Information). The products were characterized by ^{1}H NMR, ^{13}C NMR, MALDI MS, and elemental analysis data (Supporting Information).

Synthesis of 1,2,3-Triazolyl Ring-Containing Glycoconjugates of Isosteviol 65 and 66. These compounds were synthesized according to Scheme 8. To a solution of equimolar amounts of

Table 2. Binding Energy of the Lead Compounds 54, 56, and 57 in Molecular Docking Simulations

compounds	binding energy, kcal/mol
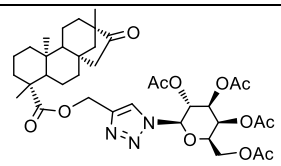 **54**	-9.3
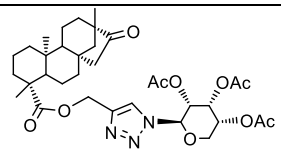 **56**	-9.6
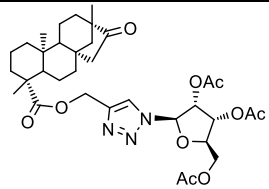 **57**	-9.4

isosteviol derivative **16** and compound **24** or **25** in a mixture of 1:1 *tert*-butanol/water was added a freshly prepared solution of equimolar amounts of sodium ascorbate in 2 mL of water and $CuSO_4 \times 5\ H_2O$ in 2 mL of water. The reaction mixture was stirred at 40 °C for 48 h, then was concentrated under reduced pressure. The residue was taken up in methylene chloride, washed successively with water, dried over anhydrous sodium sulfate, and concentrated under vacuum to provide the desired 1,2,3-triazolyl-ring-containing glycoconjugates **65** and **66** in 96% and 95% yields, respectively (Supporting Information). The

https://dx.doi.org/10.1021/acs.jnatprod.0c00134
J. Nat. Prod. XXXX, XXX, XXX−XXX

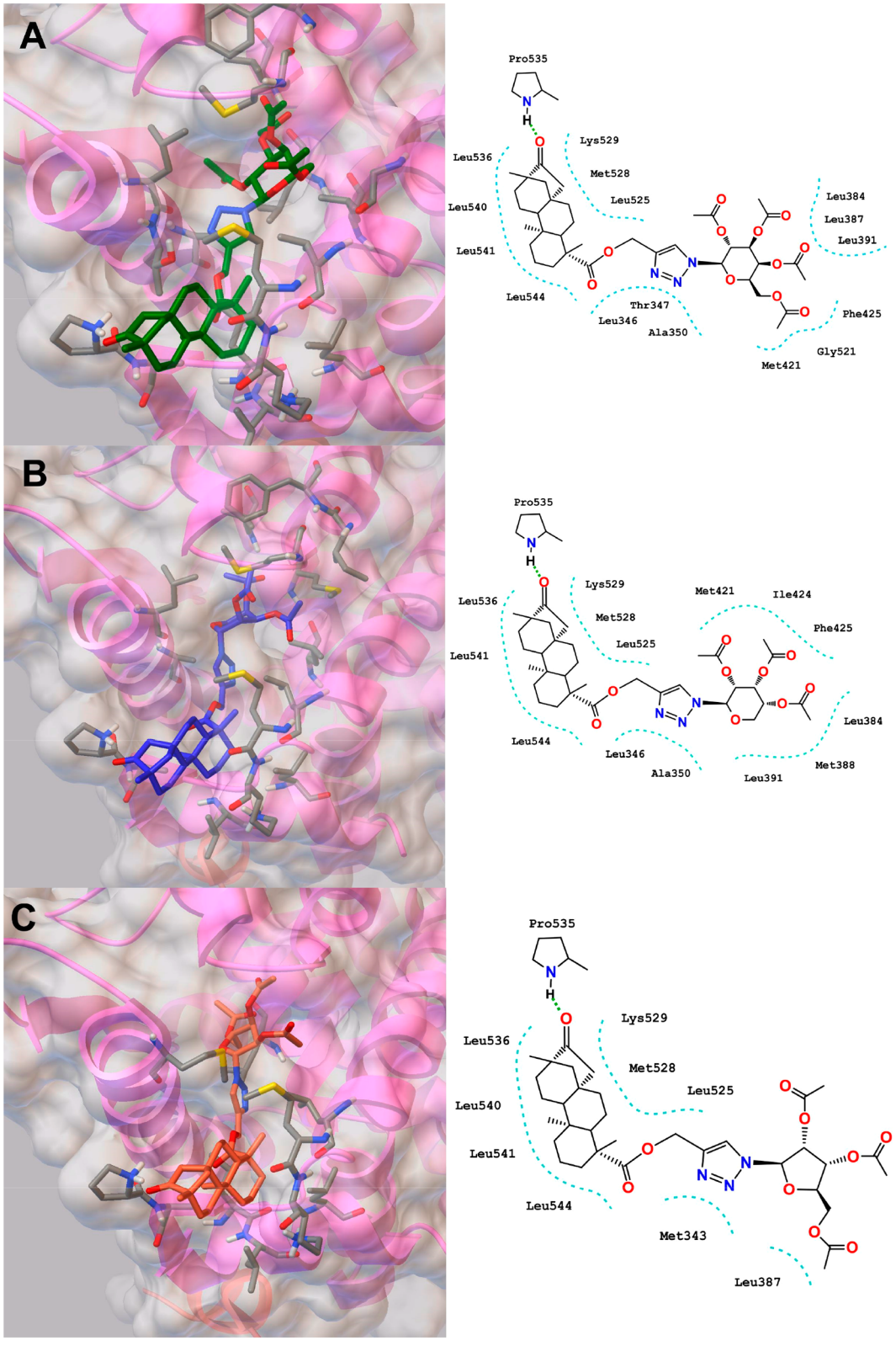

Figure 8. Molecular docking simulations and two-dimensional interaction maps of the optimized docking models of the lead compounds **54** (A), **56** (B), and **57** (C) into the ERα binding site, obtained in the lowest-energy conformation.

products were characterized by ^{1}H NMR, ^{13}C NMR, MALDI MS, and elemental analysis data (Supporting Information).

Synthesis of 1,2,3-Triazolyl-Ring-Containing Glycoconjugates of Isosteviol 67 and 68. These compounds were synthesized according to Scheme 9. To a solution of equimolar amounts of ethyl 16(*S*)-azido-*ent*-beyeran-19-oate (**20**) and compound **28** or **40** in a mixture of 1:1 *tert*-butanol/water was added a freshly prepared solution of equimolar amounts of sodium ascorbate in 2 mL of water and $CuSO_4 \times 5\ H_2O$ in 2 mL of water. The reaction mixture was stirred at 40 °C for 48 h, then was concentrated under reduced pressure. The residue was taken up in methylene chloride, washed with water, dried over anhydrous sodium sulfate, and concentrated

https://dx.doi.org/10.1021/acs.jnatprod.0c00134
J. Nat. Prod. XXXX, XXX, XXX−XXX

Scheme 9. Synthesis of 1,2,3-Triazolyl Glycoconjugates 69 and 70

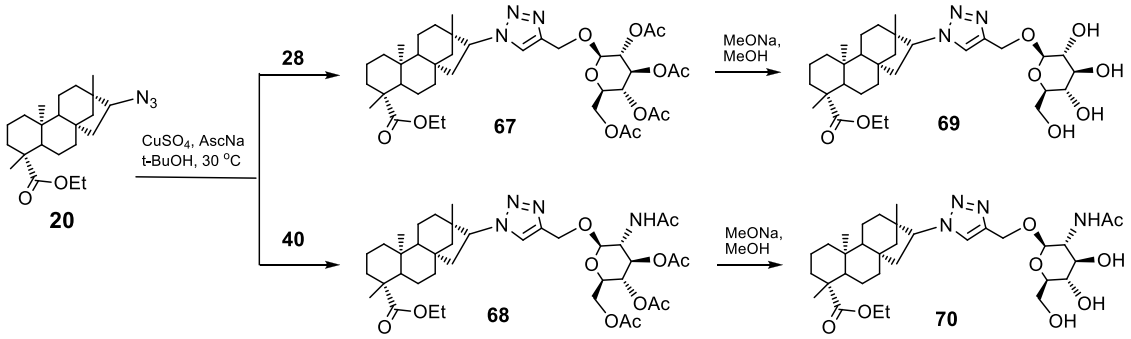

under vacuum to provide the desired 1,2,3-triazolyl-ring-containing glycoconjugates **67** and **68** with acetylated sugar residues in 79% and 69% yields, respectively (Supporting Information). The products were characterized by ^{1}H NMR, ^{13}C NMR, MALDI MS, and elemental analysis data (Supporting Information).

Synthesis of 1,2,3-Triazolyl-Ring-Containing Glycoconjugates of Isosteviol 69 and 70. These compounds were synthesized according to Scheme 9. Glycoconjugates **67** and **68** were dissolved in anhydrous MeOH at room temperature, and the pH was adjusted to 9.0 using a solution of 0.1 N MeONa/MeOH. The deacetylation procedure was monitored by TLC, and upon its completion the pH adjusted to 7.0 with the acidic ion-exchange resin Amberlyst 15. After filtration, the filtrate was concentrated under reduced pressure to afford the corresponding compounds **69** and **70** in 80% and 81% yields, respectively (pp S13, S14, Supporting Information). The products were characterized by ^{1}H NMR, ^{13}C NMR, MALDI MS, and elemental analysis data (Supporting Information).

Cytotoxicity Assay. Cytotoxic effects of the test compounds in relation to human cancer and normal cells were estimated by means of the multifunctional Cytell Cell Imaging system (GE Health Care Life Science, Sweden) using the Cell Viability Bio App, which precisely counts the number of cells and evaluates their viability from fluorescence intensity data. Two fluorescent dyes that selectively penetrate the cell membranes and fluoresce at different wavelengths were used in the experiments. The low-molecular-weight 4′,6-diamidino-2-phenylindole dye (DAPI) is able to penetrate intact membranes of living cells and color nuclei in blue. The high-molecular-weight propidium iodide dye penetrates only dead cells with damaged membranes, staining them yellow. As a result, living cells appear blue and dead cells yellow. DAPI and propidium iodide were purchased from Sigma-Aldrich. The M-HeLa clone 11 human epithelioid cervical carcinoma, a strain of HeLa, clone of M-HeLa; human breast adenocarcinoma cells (MCF-7); and WI-38 VA-13 cell culture, subline 2RA (human embryonic lung) were obtained from the Type Culture Collection of the Institute of Cytology (Russian Academy of Sciences), and the Chang liver cell line (human liver cells) was obtained from the N.F. Gamaleya Research Center of Epidemiology and Microbiology. The cells were cultured in a standard Eagle's nutrient medium manufactured at the Chumakov Institute of Poliomyelitis and Virus Encephalitis (PanEco Company) and supplemented with 10% fetal calf serum and 1% nonessential amino acids. The cells were plated into a 96-well plate (Eppendorf) at a concentration of 1×10^{5} cells/mL, with 150 μL of medium per well, and cultured in a CO_2 incubator at 37 °C. Twenty-four hours after seeding the cells into wells, each compound under study was added at a preset dilution, 150 μL to each well. The dilutions of the compounds were prepared immediately in nutrient media; 5% DMSO that does not induce the inhibition of cells at this concentration was added for better solubility. The experiments were repeated three times. Intact cells cultured in parallel with experimental cells were used as a control.

Flow Cytometry Assay. M-HeLa cells at 1×10^{6} cells/well in a final volume of 2 mL were seeded into six-well plates. After 24 h of incubation, various concentrations of test compounds were added to wells for various periods of time. For a cell apoptosis analysis, the cell were harvested at 2000 rpm for 5 min and then washed twice with ice-cold PBS, followed by resuspension in binding buffer. Next, the samples were incubated with 5 μL of annexin V-FITC and 5 μL of propidium iodide for 15 min at room temperature in the dark. Finally, the cells were analyzed by flow cytometry (Guava easyCyte, Merck, USA). The experiments were repeated three times.

Mitochondrial Membrane Potential. Cells were harvested at 2000 rpm for 5 min and then washed twice with ice-cold PBS, followed by resuspension in JC-10 (10 μg/mL) and incubation at 37 °C for 10 min. After the cells were rinsed three times and suspended in PBS, the JC-10 fluorescence was observed by flow cytometry.

Multiplex Analysis of Early Apoptosis Markers. M-HeLa cells were incubated for 24 h with each test substance. Cells were lysed in Milliplex MAP lysis buffer containing protease inhibitors; 20 μg of total protein of each lysate diluted in Milliplex MAP assay buffer 2 was analyzed according to the analysis protocol (the lysate was incubated at 4 °C overnight). The MFI was detected using the Luminex system, Merck, USA.

Statistical Analysis. The cytometric results were analyzed by the Cytell Cell Imaging multifunctional system using the Cell Viability BioApp and Apoptosis BioApp application. The data in the tables and graphs are given as the means ± standard error.

■ ASSOCIATED CONTENT

Supporting Information

The Supporting Information is available free of charge at https://pubs.acs.org/doi/10.1021/acs.jnatprod.0c00134.

Copies of ^{1}H and ^{13}C NMR spectra of all the final glycocnjugate molecules along with complete experimental procedures and characterization of the synthesized compounds; X-ray crystal data with the corresponding details (PDF)

X-ray crystal data (CIF)

X-ray crystal data (CIF)

■ AUTHOR INFORMATION

Corresponding Author

Vladimir E. Kataev − *Arbuzov Institute of Organic and Physical Chemistry, FRC Kazan Scientific Center, Russian Academy of Sciences, Kazan 420088, Russian Federation;* orcid.org/0000-0002-2767-2793; Email: kataev57@yandex.ru

Authors

Olga V. Andreeva − *Arbuzov Institute of Organic and Physical Chemistry, FRC Kazan Scientific Center, Russian Academy of Sciences, Kazan 420088, Russian Federation*

Bulat F. Garifullin − *Arbuzov Institute of Organic and Physical Chemistry, FRC Kazan Scientific Center, Russian Academy of Sciences, Kazan 420088, Russian Federation*

https://dx.doi.org/10.1021/acs.jnatprod.0c00134
J. Nat. Prod. XXXX, XXX, XXX−XXX

Radmila R. Sharipova − *Arbuzov Institute of Organic and Physical Chemistry, FRC Kazan Scientific Center, Russian Academy of Sciences, Kazan 420088, Russian Federation*
Irina Yu. Strobykina − *Arbuzov Institute of Organic and Physical Chemistry, FRC Kazan Scientific Center, Russian Academy of Sciences, Kazan 420088, Russian Federation*
Anastasiya S. Sapunova − *Arbuzov Institute of Organic and Physical Chemistry, FRC Kazan Scientific Center, Russian Academy of Sciences, Kazan 420088, Russian Federation*
Alexandra D. Voloshina − *Arbuzov Institute of Organic and Physical Chemistry, FRC Kazan Scientific Center, Russian Academy of Sciences, Kazan 420088, Russian Federation*
Mayya G. Belenok − *Arbuzov Institute of Organic and Physical Chemistry, FRC Kazan Scientific Center, Russian Academy of Sciences, Kazan 420088, Russian Federation*
Alexey B. Dobrynin − *Arbuzov Institute of Organic and Physical Chemistry, FRC Kazan Scientific Center, Russian Academy of Sciences, Kazan 420088, Russian Federation*
Leysan R. Khabibulina − *Arbuzov Institute of Organic and Physical Chemistry, FRC Kazan Scientific Center, Russian Academy of Sciences, Kazan 420088, Russian Federation*

Complete contact information is available at: https://pubs.acs.org/10.1021/acs.jnatprod.0c00134

Notes

The authors declare no competing financial interest.

■ ACKNOWLEDGMENTS

The authors are grateful to the Assigned Spectral-Analytical Center of FRC Kazan Scientific Center of RAS for technical assistance in research.

■ REFERENCES

(1) Bray, F.; Ferlay, J.; Soerjomataram, I.; Siegel, R. L.; Torre, L. A.; Jemal, A. *Ca-Cancer J. Clin.* **2018**, *68*, 394−424.
(2) Salas-Vega, S.; Iliopoulos, O.; Mossialos, E. *JAMA Oncology* **2017**, *3*, 382−390.
(3) Pethe, A. M.; Yadav, K. S. *Artif. Cells, Nanomed., Biotechnol.* **2019**, *47*, 395−405.
(4) Aleksakhina, S. N.; Kashyap, A.; Imyanitov, E. N. *Biochim. Biophys. Acta, Rev. Cancer* **2019**, *1872*, 188310.
(5) Lim, B.; Greer, Y.; Lipkowitz, S.; Takebe, N. *Cancers* **2019**, *11*, 1087.
(6) Mosettig, E.; Nes, W. R. *J. Org. Chem.* **1955**, *20*, 884−899.
(7) Khaibullin, R. N.; Strobykina, I. Yu.; Kataev, V. E.; Lodochnikova, O. A.; Gubaidullin, A. T.; Musin, R. Z. *Russ. J. Gen. Chem.* **2009**, *79*, 967−971.
(8) Kinghorn, A. D. *Stevia: The Genus Stevia. Medicinal and Aromatic Plants − Industrial Profiles*, Vol. *19*; Hardman, R., Ed.; Taylor and Francis: London, UK, 2002; p 195.
(9) (a) Mizushina, Y.; Akihisa, T.; Ukiya, M.; Hamasaki, Y.; Murakami-Nakai, C.; Kuriyama, I.; Takeuchi, T.; Sugawara, F.; Yoshida, H. *Life Sci.* **2005**, *77*, 2127−2140. (b) Kataev, V. E.; Militsina, O. I.; Strobykina, I. Yu.; Kovylyaeva, G. I.; Musin, R. Z.; Fedorova, O. V.; Rusinov, G. L.; Zueva, M. N.; Mordovskoi, G. G.; Tolstikov, A. G. *Pharm. Chem. J.* **2006**, *40*, 473−475. (c) Ma, J.; Ma, Z.; Wang, J.; Milne, R. W.; Xu, D.; Davey, A. K.; Evans, A. M. *Diabetes, Obes. Metab.* **2007**, *9*, 597−599. (d) Xu, D.; Li, L.; Wang, J.; Davey, A. K.; Zhang, S.; Evans, A. M. *Life Sci.* **2007**, *80*, 269−274. (e) Chatsudthipong, V.; Muanprasat, C. *Pharmacol. Ther.* **2009**, *121*, 41−54. (f) Takasaki, M.; Konoshima, T.; Kozuka, M.; Tokuda, H.; Takayasu, J.; Nishino, H.; Miyakoshi, M.; Mizutani, K.; Lee, K.-H. *Bioorg. Med. Chem.* **2009**, *17*, 600−605. (g) Ukiya, M.; Sawada, S.; Kikuchi, T.; Kushi, Y.; Fukatsu, M.; Akihisa, T. *Chem. Biodiversity* **2013**, *10*, 177−183. (h) Khaybullin, R. N.; Zhang, R. N.; Fu, M.; Liang, X.; Li, T.; Katritzky, A. R.; Okunieff, P.; Qi, X. *Molecules* **2014**, *19*, 18676−18689. (i) Al-Dhabi, N. A.; Arasu, M. V.; Rejiniemon, T. S. *Evid.-Based Complement. Altern. Med.* **2015**, *2015*, 164261. (j) Huang, T.-J.; Yang, C. L.; Kuo, Y. C.; Chang, Y. C.; Yang, L.-M.; Chou, B.-H.; Lin, S.-J. *Bioorg. Med. Chem.* **2015**, *23*, 720−728. (k) Strobykina, I. Yu.; Belenok, M. G.; Semenova, M. N.; Semenov, V. V.; Babaev, V. M.; Rizvanov, I. Kh.; Mironov, V. F.; Kataev, V. E. *J. Nat. Prod.* **2015**, *78*, 1300−1308. (l) Liu, C.-J.; Liu, Y.-P.; Yu, Sh.-L.; Dai, X.-J.; Zhang, T.; Tao, J.-Ch. *Bioorg. Med. Chem. Lett.* **2016**, *26*, 5455−5461. (m) Testai, L.; Strobykina, I. Yu.; Semenov, V. V.; Semenova, M.; Da Pozzo, E.; Martelli, A.; Citi, V.; Martini, C.; Breschi, M. C.; Kataev, V. E.; Calderone, V. *Int. J. Mol. Sci.* **2017**, *18*, 2060. (n) Wang, M.; Li, H.; Xu, F.; Gao, X.; Li, J.; Xu, S.; Zhang, D.; Wu, X.; Xu, J.; Hua, H.; Li, D. *Eur. J. Med. Chem.* **2018**, *56*, 885−906. (o) Sharipova, R. R.; Andreeva, O. V.; Garifullin, B. F.; Strobykina, I. Yu.; Voloshina, A. D.; Kravchenko, M. A.; Kataev, V. E. *Chem. Nat. Compd.* **2018**, *54*, 92−97. (p) Sharipova, R. R.; Belenok, M. G.; Garifullin, B. F.; Sapunova, A. S.; Voloshina, A. D.; Andreeva, O. V.; Strobykina, I. Yu.; Skvortsova, P. V.; Zuev, Yu. F.; Kataev, V. E. *MedChemComm* **2019**, *10*, 1488−1498. (q) Garifullin, B. F.; Strobykina, I. Yu.; Khabibulina, L. R.; Sapunova, A. S.; Voloshina, A. D.; Sharipova, R. R.; Khairutdinov, B. I.; Zuev, Yu. F.; Kataev, V. E. *Nat. Prod. Res.* **2019**, 1.
(10) (a) Jarrahpour, A. A.; Shekarriz, M.; Taslimi, A. *Molecules* **2004**, *9*, 29−38. (b) Filice, M.; Guisan, J. M.; Terreni, M.; Palomo, J. M. *Nat. Protoc.* **2012**, *7*, 1783−1796. (c) Bensoussan, Ch.; Rival, N.; Hanquet, G.; Colobert, F.; Reymond, S.; Cossy, J. *Tetrahedron* **2013**, *69*, 7759−7770. (d) Fusari, M.; Fallarini, S.; Lombardi, G.; Lay, L. *Bioorg. Med. Chem.* **2015**, *23*, 7439−7447. (e) Pastuch-Gawołek, G.; Malarz, K.; Mrozek-Wilczkiewicz, A.; Musioł, M.; Serda, M.; Czaplinska, B.; Musiol, R. *Eur. J. Med. Chem.* **2016**, *112*, 130−144. (f) Lutteroth, K. R.; Harris, P. W.; Wright, T. H.; Kaur, H.; Sparrow, K.; Yang, S.-H.; Cooper, G. J. S.; Brimble, M. A. *Org. Biomol. Chem.* **2017**, *15*, 5602−5608.
(11) (a) Inouye, Y.; Onodera, K.; Kitaoka, Sh.; Kirii, T. *Bull. Inst. Chem. Res. Kyoto* **1955**, *33*, 270−271. (b) Pravdić, N.; Franjić-Mihalić, I.; Danilov, B. *Carbohydr. Res.* **1975**, *45*, 302−306. (c) Lioux, T.; Busson, R.; Rozensky, J.; Nguen-Distèche, M.; Frère, J.-M.; Herdewijn, P. *Collect. Czech. Chem. Commun.* **2005**, *70*, 1615−1641. (d) Hasegawa, T.; Numata, M.; Okumura, Sh.; Kimura, T.; Sakurai, K.; Shinkai, S. *Org. Biomol. Chem.* **2007**, *5*, 2404−2412. (e) Toonstra, Ch.; Amin, M. A.; Wang, L.-X. *J. Org. Chem.* **2016**, *81*, 6176−6185.
(12) (a) Nisic, F.; Speciale, G.; Bernardi, A. *Chem. - Eur. J.* **2012**, *18*, 6895−6906. (b) Andreeva, O. V.; Belenok, M. G.; Saifina, L. F.; Shulaeva, M. M.; Dobrynin, A. B.; Sharipova, R. R.; Voloshina, A. D.; Saifina, A. F.; Gubaidullin, A. T.; Khairutdinov, B. I.; Zuev, Y. F.; Semenov, V. E.; Kataev, V. E. *Tetrahedron Lett.* **2019**, *60*, 151276.
(13) (a) Wilkinson, B. L.; Bornaghi, L. F.; Poulsen, S.-A.; Houston, T. A. *Tetrahedron* **2006**, *62*, 8115−8125. (b) Ustinov, A. V.; Stepanova, I. A.; Dubnyakova, V. V.; Zatsepin, T. S.; Nozhevnikova, E. V.; Korshun, V. A. *Russ. J. Bioorg. Chem.* **2010**, *36*, 401−445.
(14) Fan, W.-Q.; Katritzky, A. R. In *Comprehensive Heterocyclic Chemistry*; Katritzky, A. R.; Rees, C. W.; Scriven, E. F. V., Eds.; Pergamon: Oxford, UK, 1997; Vol. *4*, pp 11−14.
(15) (a) Hughes, N. A.; Kuhajda, K.-M.; Miljkovic, D. A. *Carbohydr. Res.* **1994**, *257*, 299−304. (b) Xie, D.; Zhang, J.; Yang, H.; Liu, Y.; Hu, D.; Song, B. *J. Agric. Food Chem.* **2019**, *67*, 7243−7248. (c) Sutcharitruk, W.; Sirion, Y.; Saeeng, R. *Carbohydr. Res.* **2019**, *484*, 107780. (d) Goswami, L.; Paul, S.; Kotammagari, T. K.; Bhattacharya, A. K. *New J. Chem.* **2019**, *43*, 4017−4021.
(16) (a) Elson, D. A.; Riley, R. R.; Lacey, A.; Thordarson, G.; Talamantes, F. J.; Arbeit, J. M. *Cancer. Res.* **2000**, *60*, 1267−1275. (b) Mucoz, N.; Franceschi, S.; Bosetti, C.; Moreno, V.; Herrero, R.; Smith, J. S.; Shah, K. V.; Meijer, C. J. L. M.; Bosch, F. X. *Lancet* **2002**, *359*, 1093−1101. (c) Chung, S.-H.; Lambert, P. F. *Proc. Natl. Acad. Sci. U. S. A.* **2009**, *106*, 19467−19472. (d) Xu, X.; Yang, W.; Li, Y.; Wang, Y. *Expert Opin. Drug Discovery* **2010**, *5*, 21−31. (e) Hellberg, D. *Anticancer Res.* **2012**, *32*, 3045−3054. (f) Weikum, E. R.; Liu, X.; Ortlund, E. A. *Protein Sci.* **2018**, *27*, 1876−1892. (g) Budryn, G.;

Gałązka-Czarnecka, I.; Brzozowska, E.; Grzelczyk, J.; Mostowski, R.; Żyżelewicz, D.; Cerón-Carrasco, J. P.; Pérez-Sánchez, H. *Food Chem.* **2018**, *245*, 324−336.

https://dx.doi.org/10.1021/acs.jnatprod.0c00134
J. Nat. Prod. XXXX, XXX, XXX−XXX